J. Opt. A: Pure Appl. Opt. **11** (2009) 015705 (8pp) doi:10.1088/1464-4258/11/1/015705

Scattering of a shaped beam by a spherical particle with an eccentric spherical inclusion

Bing Yan[1,3], **Xiang'e Han**[1] **and Kuan Fang Ren**[2]

[1] School of Sciences, Xidian University, Xi'an 710071, People's Republic of China
[2] UMR 6614/CORIA, CNRS–University and INSA of Rouen, France

E-mail: yanbing122530@126.com

Received 22 September 2008, accepted for publication 19 November 2008
Published 18 December 2008
Online at stacks.iop.org/JOptA/11/015705

Abstract
Based on the generalized Lorenz–Mie theory (GLMT), a method of describing a Gaussian beam scattering by an eccentric sphere is developed. For a general case, the eccentric sphere is arbitrarily located and arbitrarily oriented with respect to the illuminating Gaussian beam. The simulations are validated for plane wave scattering by an eccentric sphere and shaped beam scattering by a coated sphere. The far-field scattering and extinction efficiency factors of scattering of a Gaussian beam by an eccentric sphere in the general case of oblique illumination are discussed.

Keywords: scattering, Mie theory, laser optics, physical optics

1. Introduction

Since the invention of the laser, optical measurement techniques and optical manipulation have become very attractive research fields. The theoretical research on the interaction between light and objects is essential for the design and improvement of measurement or manipulation techniques. The scatterers encountered can be homogeneous or inhomogeneous, spherical, cylindrical, spheroidal or of a more complicated form. The incident beam can be considered as a plane wave when the scatters are very small compared to the dimensions of the incident beam. But more generally, the beam shape must be considered when the size of the scatterer is relatively large and the illumination on the scatterer is not homogeneous. Many researchers have contributed to the theory and the application of light scattering in different manners.

The most classical theory, first developed by Lorenz, Mie and Debye [7, 13, 14], treats the scattering of a spherical, isotropic, homogeneous, nonmagnetic particle illuminated by a plane wave. This theory, called the Lorenz–Mie theory (LMT), is based on the rigorous solution of Maxwell equations and so is taken as a reference in the practice of measurement technique development. In the same framework, the theory has been extended to the scattering of a plane wave by other forms of particles, such as homogeneous cylinder, spheroidal, and stratified spherical, cylindrical and spheroidal particles.

In order to take into account the inhomogeneous illumination, Gouesbet *et al* [12] have developed the generalized Lorenz–Mie theory, at the beginning for scattering of a Gaussian beam by a homogeneous sphere. This theory has then been extended to the stratified sphere [16], homogeneous cylinder [20] and spheroid [23]. In their theory, the incident beam is described by the so-called beam shape coefficients (BSCs) g_n^m in the proper coordinate system [11, 20, 22]. They have also developed very efficient algorithms to calculate these coefficients for any shaped beam [18, 19].

In the theories described above the particles always have the same symmetry as the coordinate systems chosen according to the form of the particle, i.e. spherical, cylindrical or spheroidal. But in practice, we encounter also particles with an eccentrical inclusion, such as atmospheric aerosols, chemical or biological agents [15]. Several authors have contributed to the scattering of a sphere with an eccentrical inclusion illuminated by plane waves. After Friedman *et al* [9], Stein [21] and Cruzan [5] published the addition theorem for spherical waves, providing a theoretical procedure for the solution of the eccentric problem, Fikioris *et al* [8] first obtained a mathematical expression for the scattering of an

[3] Author to whom any correspondence should be addressed.

eccentric sphere within a main sphere. Optical properties of such a particle have been studied by Borghese *et al* [4]. Ngo *et al* [15] provided a FORTRAN code for the scattering of a sphere with an eccentric inclusion illuminated by plane waves at arbitrary incidence. In order to take into account the shape of the incident beam, Gouesbet *et al* [10] presented a formulation in the framework of GLMT, but without numerical results.

Based on the preceding work, we present in this paper a general scattering theory of an arbitrary shaped beam by a sphere with an eccentric inclusion in the framework of GLMT. The emphasis will be made on the coincidence of the vector functions, the addition theorem and the beam shape coefficients. After validation of our theory and the code, numerical results will be presented to show some particular scattering characteristics of such a particle.

The body of this paper proceeds as follows. In section 2, the description of the incident beam in spherical coordinates is given and the BSC evaluation method, calculations of far-field scattering as well as extinction and scattering cross sections provided. The numerical results of the formulae are verified and discussed in section 3 and, as general cases, the scattering for a Gaussian beam in oblique illumination by an eccentric sphere is also given. Section 4 is devoted to the conclusion.

2. Scattering theory

2.1. Geometry of the scattering system

We consider a sphere (called the main sphere hereafter) located at the center of the coordinate system $O_1 - x_1y_1z_1$ with a spherical inclusion of the center on the z_1 axis at $z_1 = d$. The three axes of the coordinate system O_1–$x_2y_2z_2$ attached to the inclusion are respectively parallel to the main coordinate system O_1–$x_1y_1z_1$ (figure 1(a)). The radii and refractive indexes of the main sphere and the inclusion are respectively a, m_1 and b, m_2. We suppose that the main sphere encloses completely the inclusion sphere so that $|d| < a$. The wavenumbers in the main sphere and in the inclusion are respectively k_1 and k_2. The surrounding medium of refractive index m_0 is non-absorbing.

2.2. Incident beam

A shaped beam with arbitrary orientation and position illuminates the particle. The center of the beam is located at $O_G(x_0, y_0, z_0)$ in the coordinate system $O_1 - x_1y_1z_1$. The main propagation direction makes a angle β to the axis z_1 (figure 1(b)). We suppose that the incident waves are monochromatic with a time dependence as $\exp(\mathrm{i}\omega t)$, where ω is the angular frequency, and will be omitted from all formulae as in normal practice.

The incident beam can be expanded in terms of spherical vector wavefunctions $\bar{\mathbf{m}}^{(1)}_{nm,1}(kr_1, \theta_1, \phi_1)$ and $\bar{\mathbf{n}}^{(1)}_{nm,1}(kr_1, \theta_1, \phi_1)$ (see appendix A for their expressions) as [12]

$$\mathbf{E}_i = E_0 \sum_{n=1}^{\infty} \sum_{m=-n}^{n} C_n [g^m_{n,TM} \bar{\mathbf{n}}^{(1)}_{nm,1}(kr_1, \theta_1, \phi_1) - \mathrm{i} g^m_{n,TE} \bar{\mathbf{m}}^{(1)}_{nm,1}(kr_1, \theta_1, \phi_1)], \quad (1)$$

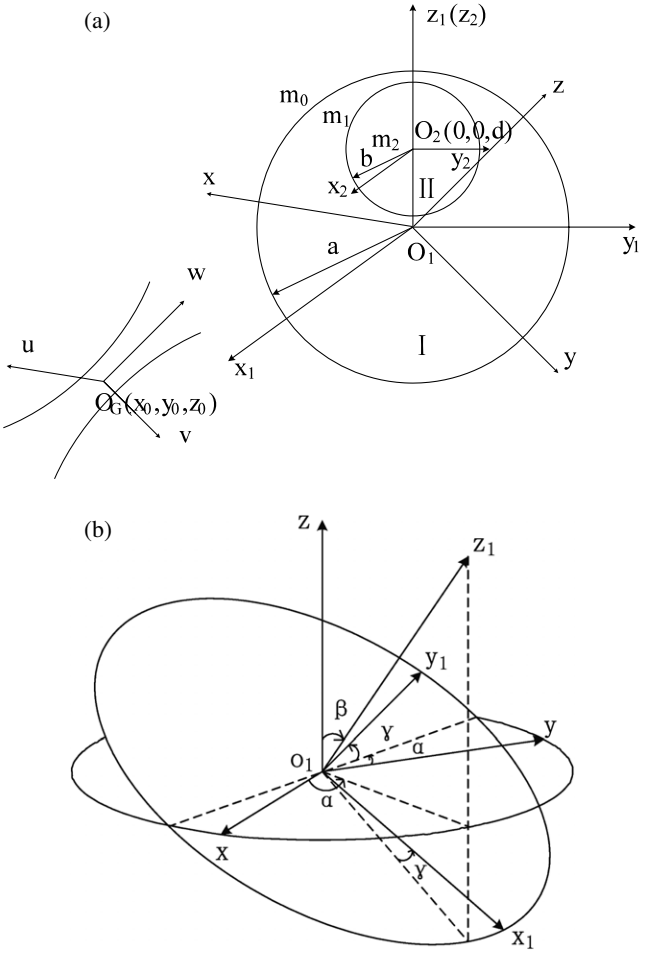

Figure 1. Scattering geometry of the problem. (b) Euler angles of rotation α, β and γ for transforming the O_1–xyz coordinate system into the O_1–$x_1y_1z_1$ coordinate system. Parallel Cartesian coordinate systems O_1–xyz and $O_G - uvw$ are attached to the main sphere and to the beam center, respectively.

where E_0 is the amplitude of the electric field at the center of the incident beam, the number 1 in the subscript denotes that the vector functions are expressed in the coordinate system O_1–$x_1y_1z_1$ and the coordinates will be omitted in the following sections if there is no confusion. The coefficient is

$$C_n = (-\mathrm{i})^{n+1} \frac{2n+1}{n(n+1)}. \quad (2)$$

In the framework of GLMT, the two series BSCs can be evaluated by the quadrature method according to the radial component of electric $E_r(r, \theta, \phi)$ and magnetic $H_r(r, \theta, \phi)$ fields:

$$g^m_{n,TM} = \frac{kr\mathrm{i}^{n+1}}{4\pi j_n(kr)} \frac{(n-|m|)!}{(n+|m|)!} \int_0^{2\pi} \int_0^{\pi} \frac{E_r(r, \theta, \phi)}{E_0} \times P_n^{|m|}(\cos\theta) \mathrm{e}^{-\mathrm{i}m\phi} \sin\theta \, \mathrm{d}\theta \, \mathrm{d}\phi, \quad (3)$$

$$g^m_{n,TE} = \frac{kr\mathrm{i}^{n+1}}{4\pi j_n(kr)} \frac{(n-|m|)!}{(n+|m|)!} \int_0^{2\pi} \int_0^{\pi} \frac{H_r(r, \theta, \phi)}{H_0} \times P_n^{|m|}(\cos\theta) \mathrm{e}^{-\mathrm{i}m\phi} \sin\theta \, \mathrm{d}\theta \, \mathrm{d}\phi, \quad (4)$$

where $j_n(r)$ is the spherical Bessel function. Theoretically, the value of r can be chosen arbitrarily. But in practice it

should be correctly chosen in order to ensure a rapid numerical conversion. Ren has shown that the best choice is $kr = n + 1/2$ [19]. If the analytical expression of the incident beam in its proper coordinate system, such as for a Gaussian beam or Gaussian-like beam [1, 2, 6], is known, the radial components $E_r(r, \theta, \phi)$ and $H_r(r, \theta, \phi)$ in the main sphere coordinate system can be obtained by coordinate translation and rotation [22].

In the case where the incident beam propagation direction is parallel to the axis z_1, the integral localized approximation can be used for an arbitrary shaped beam to accelerate the calculation:

$$g^m_{n,TM} = \frac{Z^m_n}{2\pi E_0}\int_0^{2\pi} \bar{E}_r\left(kr = n+\frac{1}{2}, \theta = \frac{\pi}{2}, \phi'\right) \times \exp(-\mathrm{i}m\phi')\,\mathrm{d}\phi', \tag{5}$$

$$g^m_{n,TE} = \frac{Z^m_n}{2\pi H_0}\int_0^{2\pi} \bar{H}_r\left(kr = n+\frac{1}{2}, \theta = \frac{\pi}{2}, \phi'\right) \times \exp(-\mathrm{i}m\phi')\,\mathrm{d}\phi', \tag{6}$$

where $\bar{E}_r$ and $\bar{H}_r$ are the same as E_r and H_r, respectively, except that kr is replaced by $(n + \frac{1}{2})$ and θ by $\pi/2$. The factor Z^m_n is given by

$$Z^m_n = \begin{cases} \dfrac{2n(n+1)}{2n+1} & m = 0 \\ \left(\dfrac{-2\mathrm{i}}{2n+1}\right)^{|m|-1} & m \neq 0. \end{cases} \tag{7}$$

For example, the beam shape coefficients of a Gaussian beam can be obtained by

$$\begin{aligned}\begin{pmatrix} g^m_{n,TM} \\ \mathrm{i}g^m_{n,TE}\end{pmatrix} &= \mathrm{i}Q\frac{Z^m_n}{4\pi}\mathrm{e}^{-\mathrm{i}Q\gamma^2+\mathrm{i}kz_0} \\ &\times \int_0^{2\pi} \mathrm{e}^{2\mathrm{i}Q\rho_n(\xi_0\cos\phi+\eta_0\sin\phi)}[\mathrm{e}^{-\mathrm{i}(m-1)} \pm \mathrm{e}^{-\mathrm{i}(m+1)}]\,\mathrm{d}\phi \\ &= \mathrm{i}Q\frac{Z^m_n}{2}\mathrm{e}^{-\mathrm{i}Q\gamma^2+\mathrm{i}kz_0}[\mathrm{e}^{\mathrm{i}(m-1)\phi_0}J_{m-1}(2Q\rho_n\rho_0) \\ &\pm \mathrm{e}^{\mathrm{i}(m+1)\phi_0}J_{m+1}(2Q\rho_n\rho_0)],\end{aligned} \tag{8}$$

where

$$Q = \frac{1}{\mathrm{i}-2z_0/l}, \qquad l = k\omega_0^2, \qquad s = \frac{1}{k\omega_0}, \tag{9}$$

$$\rho_n = (n+1/2)s, \qquad \gamma = \sqrt{\rho_n^2+\rho_0^2}, \qquad \xi_0 = x_0/\omega_0, \quad \eta_0 = y_0/\omega_0, \tag{10}$$

x_0, y_0, z_0 are the coordinates of the beam center in $O_1 - x_1y_1z_1$ and ω_0 is the beam-waist radius. The evaluation of the BSCs by the integral localized approximation being very fast, an alternative method to obtain the BSCs in the main sphere coordinates is to calculate the BSCs in the coordinate system parallel to that of the beam but centered at O by equations (3) and (4), and then to obtain the BSCs in the main sphere by utilization of the addition theorem for rotation from the BSCs obtained.

2.3. Main sphere

We examine now the fields outside and inside the main sphere. The scattered fields $\mathbf{E}^1_{sca}$ can be expanded in terms of vector functions by using the spherical Bessel functions of the fourth kind [12]:

$$\mathbf{E}^1_{sca} = E_0\sum_{n=1}^{\infty}\sum_{m=-n}^{n} C_n[\mathrm{i}b^m_n g^m_{n,TE}\bar{\mathbf{m}}^{(4)}_{nm,1} - a^m_n g^m_{n,TM}\bar{\mathbf{n}}^{(4)}_{nm,1}]. \tag{11}$$

The scattering coefficients a^m_n and b^m_n are determined by invoking boundary conditions (i) at the surface of the inclusion and (ii) at the surface of the main sphere.

Similarly, the internal fields $\mathbf{E}^1_{sph}$ can be expanded in terms of vector functions by using spherical Bessel functions of the third and fourth kinds:

$$\mathbf{E}^1_{sph} = E_0\sum_{n=1}^{\infty}\sum_{m=-n}^{n} C_n[c^m_n\bar{\mathbf{n}}^{(4)}_{nm,1} - \mathrm{i}d^m_n\bar{\mathbf{m}}^{(4)}_{nm,1} + e^m_n\bar{\mathbf{n}}^{(3)}_{nm,1} - \mathrm{i}f^m_n\bar{\mathbf{m}}^{(3)}_{nm,1}]. \tag{12}$$

Applying boundary conditions at the main sphere surface yields the following four sets of equations:

$$g^m_{n,TE}\psi_n(ka) - b^m_n g^m_{n,TE}\xi^{(2)}_n(ka) = \frac{k}{k_1}[d^m_n\xi^{(2)}_n(k_1a) + f^m_n\xi^{(1)}_n(k_1a)], \tag{13}$$

$$g^m_{n,TE}\psi'_n(ka) - b^m_n g^m_{n,TE}\xi^{'(2)}_n(ka) = d^m_n\xi^{'(2)}_n(k_1a) + f^m_n\xi^{'(1)}_n(k_1a), \tag{14}$$

$$g^m_{n,TM}\psi_n(ka) - a^m_n g^m_{n,TM}\xi^{(2)}_n(ka) = c^m_n\xi^{(2)}_n(k_1a) + e^m_n\xi^{(1)}_n(k_1a), \tag{15}$$

$$g^m_{n,TM}\psi'_n(ka) - a^m_n g^m_{n,TM}\xi^{'(2)}_n(ka) = \frac{k}{k_1}[c^m_n\xi^{'(2)}_n(k_1a) + e^m_n\xi^{'(1)}_n(k_1a)], \tag{16}$$

where $\psi_n(r)$ and $\xi^{(q)}_n(r)(q = 1, 2)$ are the Riccati–Bessel functions defined by

$$\psi_n(r) = rj_n(r) \qquad \text{and} \qquad \xi^{(q)}_n(r) = rh^{(q)}_n(r)$$

and the primes denote derivatives with respect to the argument.

2.4. Inclusion sphere

The fields inside and outside the inclusion can be expanded [12] in the coordinate system O_2–$x_2y_2z_2$ as

$$\mathbf{E}^2_{int}(\mathbf{r}_2) = E_0\sum_{n=1}^{\infty}\sum_{m=-n}^{n} C_n[p^m_n\bar{\mathbf{n}}^{(1)}_{nm,2} - \mathrm{i}q^m_n\bar{\mathbf{m}}^{(1)}_{nm,2}], \tag{17}$$

$$\mathbf{E}^2_{ext}(\mathbf{r}_2) = E_0\sum_{n=1}^{\infty}\sum_{m=-n}^{n} C_n[r^m_n\bar{\mathbf{n}}^{(4)}_{nm,2} - \mathrm{i}s^m_n\bar{\mathbf{m}}^{(4)}_{nm,2} + t^m_n\bar{\mathbf{n}}^{(3)}_{nm,2} - \mathrm{i}u^m_n\bar{\mathbf{m}}^{(3)}_{nm,2}]. \tag{18}$$

The application of the boundary conditions at the surface of the inclusion $|r_2| = b$ yields the following four sets of equations:

$$q^m_n\psi_n(k_2b) = \frac{k_2}{k_1}[s^m_n\xi^{(2)}_n(k_1b) + u^m_n\xi^{(1)}_n(k_1b)], \tag{19}$$

$$q^m_n\psi'_n(k_2b) = s^m_n\xi^{'(2)}_n(k_1b) + u^m_n\xi^{'(1)}_n(k_1b), \tag{20}$$

$$p^m_n\psi_n(k_2b) = r^m_n\xi^{(2)}_n(k_1b) + t^m_n\xi^{(1)}_n(k_1b), \tag{21}$$

$$p_n^m \psi_n'(k_2 b) = \frac{k_2}{k_1}[r_n^m \xi_n^{'(2)}(k_1 b) + t_n^m \xi_n^{'(1)}(k_1 b)]. \quad (22)$$

After a little bit of algebra, we can find the relationship between the interior and exterior field coefficients:

$$Q_n^{\mathrm{r}} = \frac{t_n^m}{r_n^m} = \frac{k_2 \xi_n^{'(2)}(k_1 b)\psi_n(k_2 b) - k_1 \xi_n^{(2)}(k_1 b)\psi_n'(k_2 b)}{k_1 \xi_n^{(1)}(k_1 b)\psi_n'(k_2 b) - k_2 \xi_n^{'(1)}(k_1 b)\psi_n(k_2 b)}, \quad (23)$$

$$Q_n^{\mathrm{s}} = \frac{u_n^m}{s_n^m} = \frac{k_1 \xi_n^{'(2)}(k_1 b)\psi_n(k_2 b) - k_2 \xi_n^{(2)}(k_1 b)\psi_n'(k_2 b)}{k_2 \xi_n^{(1)}(k_1 b)\psi_n'(k_2 b) - k_1 \xi_n^{'(1)}(k_1 b)\psi_n(k_2 b)}. \quad (24)$$

The coefficients Q_n^{r} and Q_n^{s} contain the information of the inclusion sphere such as its size and refractive index.

2.5. Fields interior to the main sphere

Until now the fields between the inclusion surface and the main sphere surface are expressed in two different coordinate systems. To find the relations between the two expressions the addition theorem must be applied. Stein [21] and Cruzan [5] have derived the translation addition theorems for the vector spherical functions which permit us to express the coefficients c_n^m, d_n^m, e_n^m and f_n^m in terms of the coefficients r_n^m, s_n^m, t_n^m and u_n^m:

$$\bar{\mathbf{m}}_{nm,2}^{(q)}(k\mathbf{r}_2) = \sum_{n'=1}^{\infty}[\bar{A}_{nn'}^m \bar{\mathbf{m}}_{n'm,1}^{(q)}(k\mathbf{r}_1) + \bar{B}_{nn'}^m \bar{\mathbf{n}}_{n'm,1}^{(q)}(k\mathbf{r}_1)], \quad (25)$$

$$\bar{\mathbf{n}}_{nm,2}^{(q)}(k\mathbf{r}_2) = \sum_{n'=1}^{\infty}[\bar{A}_{nn'}^m \bar{\mathbf{n}}_{n'm,1}^{(q)}(k\mathbf{r}_1) + \bar{B}_{nn'}^m \bar{\mathbf{m}}_{n'm,1}^{(q)}(k\mathbf{r}_1)], \quad (26)$$

where $q = 1, 2, 3, 4$ denote the order of the spherical Bessel functions. The translation coefficients $\bar{A}_{nn'}^m$ and $\bar{B}_{nn'}^m$ are given in appendix B. It is worth noting that the coefficients $\bar{A}_{nn'}^m$ and $\bar{B}_{nn'}^m$ are independent of the kind of Bessel function, so no difference is made as in [15].

By using equations (12), (17), (25) and (26), we obtain the relations between the coefficients in the two different coordinate systems:

$$C_n c_n^m = \sum_{n'=1}^{\infty} C_{n'}(r_{n'}^m \bar{A}_{nn'}^m - \mathrm{i} s_{n'}^m \bar{B}_{nn'}^m), \quad (27)$$

$$C_n d_n^m = \sum_{n'=1}^{\infty} C_{n'}(s_{n'}^m \bar{A}_{nn'}^m + \mathrm{i} r_{n'}^m \bar{B}_{nn'}^m), \quad (28)$$

$$C_n e_n^m = \sum_{n'=1}^{\infty} C_{n'}(t_{n'}^m \bar{A}_{nn'}^m - \mathrm{i} u_{n'}^m \bar{B}_{nn'}^m), \quad (29)$$

$$C_n f_n^m = \sum_{n'=1}^{\infty} C_{n'}(u_{n'}^m \bar{A}_{nn'}^m + \mathrm{i} t_{n'}^m \bar{B}_{nn'}^m). \quad (30)$$

Substituting these equations into equations (13)–(16) together with equations (23) and (24) yields the following four sets of equations:

$$C_n g_{n,TM}^m[\psi_n(ka) - a_n^m \xi_n^{(2)}(ka)] = \sum_{n'=1}^{\infty}[C_{n'} r_{n'}^m \bar{A}_{nn'}^m(\xi_n^{(2)}(k_1 a) + Q_{n'}^r \xi_n^{(1)}(k_1 a)) - \mathrm{i} C_{n'} s_{n'}^m \bar{B}_{nn'}^m(\xi_n^{(2)}(k_1 a) + Q_{n'}^s \xi_n^{(1)}(k_1 a))], \quad (31)$$

$$C_n g_{n,TM}^m[\psi_n'(ka) - a_n^m \xi_n^{'(2)}(ka)] = \frac{k}{k_1}\sum_{n'=1}^{\infty}[C_{n'} r_{n'}^m \bar{A}_{nn'}^m(\xi_n^{'(2)}(k_1 a) + Q_{n'}^r \xi_n^{'(1)}(k_1 a)) - \mathrm{i} C_{n'} s_{n'}^m \bar{B}_{nn'}^m(\xi_n^{'(2)}(k_1 a) + Q_{n'}^s \xi_n^{'(1)}(k_1 a))], \quad (32)$$

$$C_n g_{n,TE}^m[\psi_n(ka) - b_n^m \xi_n^{(2)}(ka)] = \frac{k}{k_1}\sum_{n'=1}^{\infty}[C_{n'} s_{n'}^m \bar{A}_{nn'}^m(\xi_n^{(2)}(k_1 a) + Q_{n'}^s \xi_n^{(1)}(k_1 a)) + \mathrm{i} C_{n'} r_{n'}^m \bar{B}_{nn'}^m(\xi_n^{(2)}(k_1 a) + Q_{n'}^r \xi_n^{(1)}(k_1 a))], \quad (33)$$

$$C_n g_{n,TE}^m[\psi_n'(ka) - b_n^m \xi_n^{'(2)}(ka)] = \sum_{n'=1}^{\infty}[C_{n'} s_{n'}^m \bar{A}_{nn'}^m(\xi_n^{'(2)}(k_1 a) + Q_{n'}^s \xi_n^{'(1)}(k_1 a)) + \mathrm{i} C_{n'} r_{n'}^m \bar{B}_{nn'}^m(\xi_n^{'(2)}(k_1 a) + Q_{n'}^r \xi_n^{'(1)}(k_1 a))]. \quad (34)$$

2.6. Scattering coefficients

The scattering coefficients a_n^m and b_n^m as well as the internal field coefficients t_n^m and u_n^m of the main sphere can be solved from these equations:

$$C_n g_{n,TE}^m \gamma_n = \sum_{n'=1}^{\infty} C_{n'}[s_{n'}^m S_{nn'}^{m,(1)} + \mathrm{i} r_{n'}^m R_{nn'}^{m,(1)}], \quad (35)$$

$$C_n g_{n,TM}^m \gamma_n = \sum_{n'=1}^{\infty} C_{n'}[r_{n'}^m R_{nn'}^{m,(2)} - \mathrm{i} s_{n'}^m S_{nn'}^{m,(2)}], \quad (36)$$

where

$$\gamma_n = k_1[\psi_n(ka)\xi_n^{'(2)}(ka) - \psi_n'(ka)\xi_n^{(2)}(ka)], \quad (37)$$

$$R_{nn'}^{m,(1)} = \bar{B}_{nn'}^m\{k\xi_n^{'(2)}(ka)[\xi_n^{(2)}(k_1 a) + Q_{n'}^r \xi_n^{(1)}(k_1 a)] - k_1 \xi_n^{(2)}(ka)[\xi_n^{'(2)}(k_1 a) + Q_{n'}^r \xi_n^{'(1)}(k_1 a)]\}, \quad (38)$$

$$R_{nn'}^{m,(2)} = \bar{A}_{nn'}^m\{k_1 \xi_n^{'(2)}(ka)[\xi_n^{(2)}(k_1 a) + Q_{n'}^r \xi_n^{(1)}(k_1 a)] - k\xi_n^{(2)}(ka)[\xi_n^{'(2)}(k_1 a) + Q_{n'}^r \xi_n^{'(1)}(k_1 a)]\}, \quad (39)$$

$$S_{nn'}^{m,(1)} = \bar{A}_{nn'}^m\{k\xi_n^{'(2)}(ka)[\xi_n^{(2)}(k_1 a) + Q_{n'}^s \xi_n^{(1)}(k_1 a)] - k_1 \xi_n^{(2)}(ka)[\xi_n^{'(2)}(k_1 a) + Q_{n'}^s \xi_n^{'(1)}(k_1 a)]\}, \quad (40)$$

$$S_{nn'}^{m,(2)} = \bar{B}_{nn'}^m\{k_1 \xi_n^{'(2)}(ka)[\xi_n^{(2)}(k_1 a) + Q_{n'}^s \xi_n^{(1)}(k_1 a)] - k\xi_n^{(2)}(ka)[\xi_n^{'(2)}(k_1 a) + Q_{n'}^s \xi_n^{'(1)}(k_1 a)]\}. \quad (41)$$

The scattering coefficients can then be calculated by using equations (31) and (32).

2.7. Scattering waves in far-field

In the far-field from the scatterer $kr_1 \gg ka$, the spherical Hankel function reduces to spherical waves:

$$h_n^{(1)}(kr) \sim (-\mathrm{i})^n \frac{\mathrm{e}^{\mathrm{i}kr}}{\mathrm{i}kr}, \qquad h_n^{(2)}(kr) \sim \mathrm{i}^{n+1} \frac{\mathrm{e}^{-\mathrm{i}kr}}{kr}. \quad (42)$$

The scattered fields are therefore transversal spherical waves and the nonzero components simplify to [12]

$$E_\theta^s = \mathrm{i}E_0 \frac{\mathrm{e}^{-\mathrm{i}kr}}{kr} \sum_{n=1}^{\infty} \sum_{m=-n}^{n} \frac{2n+1}{n(n+1)} \times [a_n^m g_{n,TM}^m \tau_n^{|m|} + \mathrm{i}m b_n^m g_{n,TE}^m \pi_n^{|m|}] \exp(\mathrm{i}m\phi), \quad (43)$$

$$E_\phi^s = -E_0 \frac{\mathrm{e}^{-\mathrm{i}kr}}{kr} \sum_{n=1}^{\infty} \sum_{m=-n}^{n} \frac{2n+1}{n(n+1)} \times [m a_n^m g_{n,TM}^m \pi_n^{|m|} + \mathrm{i} b_n^m g_{n,TE}^m \tau_n^{|m|}] \exp(\mathrm{i}m\phi). \quad (44)$$

The scattering and extinction cross sections can be obtained by a similar procedure as for a spherical particle [12] and they can be expressed as

$$C_{\mathrm{sca}} = \frac{\lambda^2}{2\pi} \sum_{n=1}^{\infty} \sum_{m=-n}^{n} \frac{2n+1}{n(n+1)} \frac{(n+|m|)!}{(n-|m|)!} \times (|a_n^m|^2 |g_{n,TM}^m|^2 + |b_n^m|^2 |g_{n,TE}^m|^2), \quad (45)$$

$$C_{\mathrm{ext}} = \frac{\lambda^2}{2\pi} \mathrm{Re} \sum_{n=1}^{\infty} \sum_{m=-n}^{n} \frac{2n+1}{n(n+1)} \frac{(n+|m|)!}{(n-|m|)!} \times [a_n^m |g_{n,TM}^m|^2 + b_n^m |g_{n,TE}^m|^2], \quad (46)$$

$$C_{\mathrm{abs}} = C_{\mathrm{ext}} - C_{\mathrm{sca}}. \quad (47)$$

It is worth noting that the expressions for scattering and cross sections are similar to those for a spherical particle due to the fact that the product of the same m appears for the scattering coefficients a_n^m, b_n^m and the beam shape coefficients $g_{n,TM}^m$, $g_{n,TE}^m$. However, the formulae of radiation pressure are quite different because the scattering and beam shape coefficients of different m intervene, which will be discussed elsewhere.

3. Numerical results and discussion

3.1. Scattering intensities

In order to validate our formulation and code, we compare the scattering diagrams calculated by our code with the published results in special cases.

When $d = 0$ an eccentric sphere becomes a coated sphere and we have compared the numerical results predicted by our code and those obtained by GLMT with different beam parameters such as position, focalization and polarization, and particle properties such as size and refractive index. The agreement is always excellent. The results are not presented here for the sake of conciseness.

It is well known that when the beam-waist radius is sufficiently larger than the radius of the sphere, the result for the Gaussian beam scattering is identical to that for the case of plane wave incidence. As an example, an eccentric sphere with the same parameters as in figure 4 of [8], i.e. $ka = 3.0$, $kb = 1.0$, $kd = 2.0$, $m_1 = 1.3$ and $m_2 = 1.7$, is assumed to be illuminated by a Gaussian beam. The beam-waist radius is $w_0 = 3.0\ \mu$m, so very much larger than the particle size, and the incident angles are $\alpha = \gamma = 0°$ and $\beta = 90°$. The scattering intensities obtained by our code are compared with figure 4 in [8]. As shown in figure 2, the agreement is satisfactory.

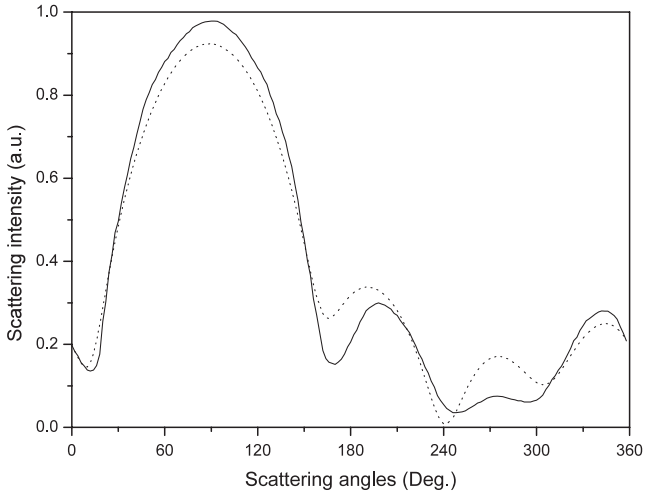

Figure 2. Comparison of the scattering intensities obtained by our code (dashed line) and those published in [8] (solid line).

Furthermore, we have simulated the scattering diagrams of a coated sphere illuminated at $x_0 = y_0 = z_0 = 0\ \mu$m by a Gaussian beam. The wavelength and the beam waist are, respectively, $\lambda = 0.6328\ \mu$m and $w_0 = 1.5\ \mu$m. The scattering diagrams of the angle set $\alpha = \beta = \gamma = 0°$ are compared with those of the angle set $\alpha = \gamma = 0°$, $\beta = 60°$. As found in figure 3, the scattering patterns show good coincidence except for an angular shift of β toward the left side, as is expected.

When an eccentric sphere is illuminated obliquely by a Gaussian beam, not only the peaks are shifted but the patterns are also modified according to the beam shape. We consider a glycerol droplet containing a glass inclusion in the air illuminated by a Gaussian beam. The parameters of the particle are $a = 2.0\ \mu$m, $b = 1.0\ \mu$m, $m_1 = 1.4746$, $m_2 = 1.94$ and $d = 0.5\ \mu$m. The Gaussian beam ($w_0 = 1.0\ \mu$m, $\lambda = 0.5145\ \mu$m) is centered at the origin of the coordinate system $O_1 - x_1 y_1 z_1$. The incident angles are $\alpha = \gamma = 0°$, and $\beta = 60°$. Two curves are plotted in figure 4 for i_φ and i_θ.

3.2. Efficiency sections

The scattering and extinction efficiency are important in the optical measurement. We show in this section the numerical results obtained by our code.

Examples of results are provided in table 1, which compares scattering and extinction efficiency factors evaluated by coated sphere theory and our eccentric method. By changing the radii, three kinds of coated spheres with the parameters $m_1 = 1.409 - 0.1747\mathrm{i}$, $m_2 = 1.59 - 0.66\mathrm{i}$ are considered and two sets of data are obtained. The first set of data are obtained by using the concentric sphere code presented in Bohren and Huffman [17]. The second set of data is obtained by using our eccentric method as $d = 0.0\ \mu$m, $w_0 = 200\ \mu$m ($w_0 \gg a$), $x_0 = y_0 = z_0 = 0.0\ \mu$m and $\alpha = \beta = 0°$. For the current cases the agreement is satisfactory.

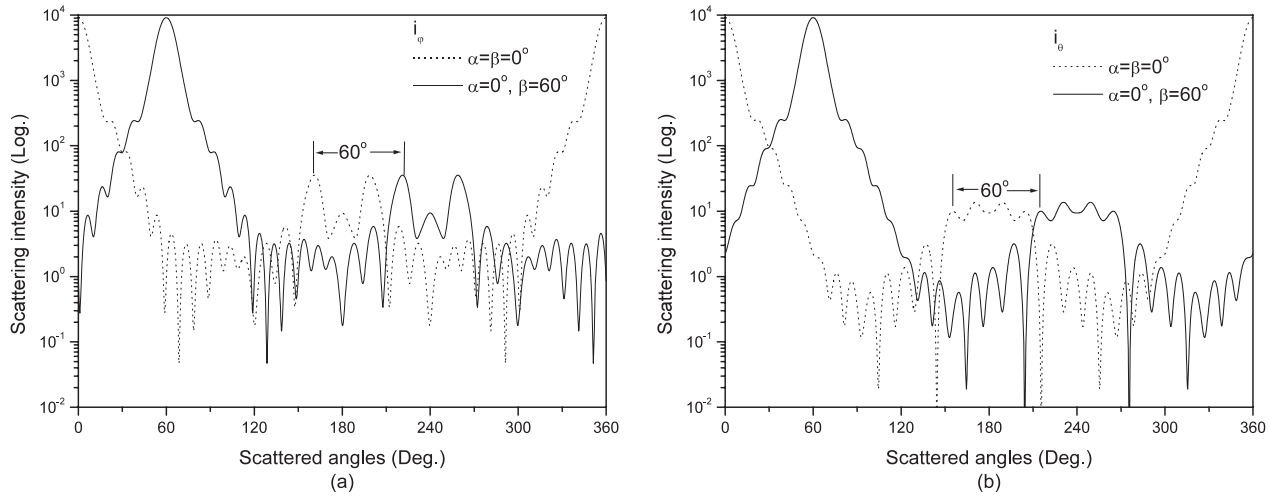

Figure 3. Scattering diagrams of a coated sphere illuminated by a Gaussian beam ($w_0 = 1.5\ \mu$m, $\lambda = 0.6328\ \mu$m, $x_0 = y_0 = z_0 = 0\ \mu$m) for two angle sets $\alpha = \beta = \gamma = 0°$ and $\alpha = \gamma = 0°$, $\beta = 60°$ for i_φ (a) and i_θ (b). The radii and the refractive index of the particle are, respectively, $a = 2.0\ \mu$m, $b = 1.0\ \mu$m, $m_1 = 1.3699$ and $m_2 = 1.3965$.

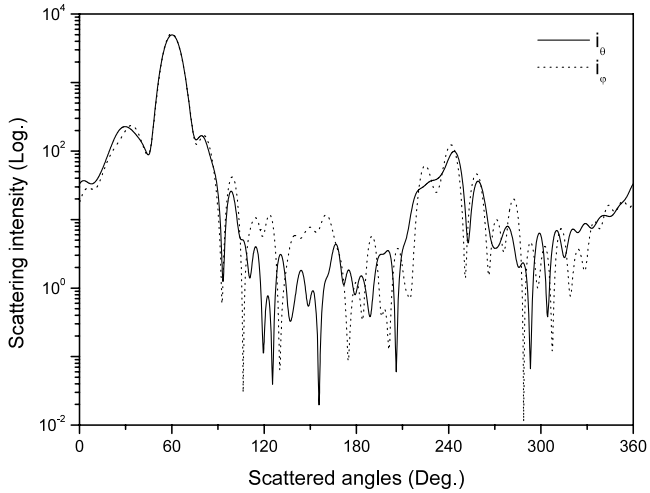

Figure 4. Scattering diagrams of an eccentric sphere illuminated by a Gaussian beam ($w_0 = 1.0\ \mu$m, $\lambda = 0.5145\ \mu$m, $x_0 = y_0 = z_0 = 0\ \mu$m) at $\alpha = \gamma = 0°$ and $\beta = 60°$. The radii, the refractive index and distance between centers of the particle are, respectively, $a = 2.0\ \mu$m, $b = 1.0\ \mu$m, $m_1 = 1.4746$, $m_2 = 1.94$ and $d = 0.5\ \mu$m.

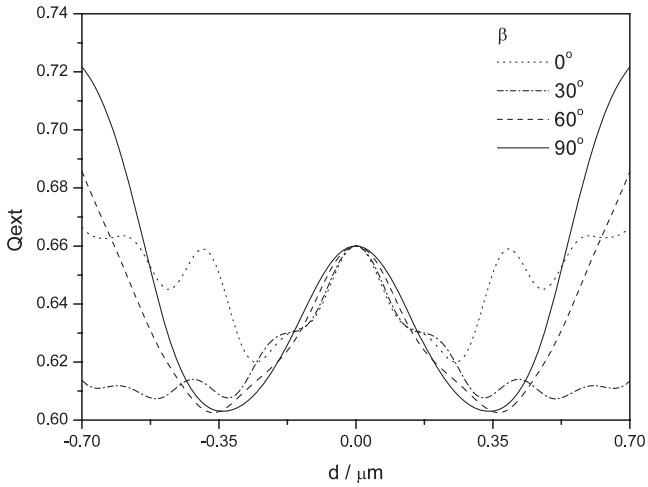

Figure 5. Extinction efficiency factor versus the eccentric distance. A 2.0 μm diameter glycerol droplet ($m_1 = 1.4746$) containing a 0.5 μm diameter glass inclusion ($m_2 = 1.94$) is illuminated by a Gaussian beam ($w_0 = 0.8\ \mu$m, $\lambda = 0.5145\ \mu$m, $x_0 = y_0 = z_0 = 0\ \mu$m) at different incidence angles ($\alpha = \gamma = 0°$).

Figure 5 shows the extinction efficiencies as a function of displacement distance d for a 2.0 μm diameter glycerol droplet ($m_1 = 1.4746$) containing a 0.5 μm diameter glass inclusion ($m_2 = 1.94$). The particle is assumed to be located in air ($m_0 = 1.0$). The parameters of the Gaussian beam are $w_0 = 0.8\ \mu$m, $\lambda_0 = 0.5145\ \mu$m, $x_0 = y_0 = z_0 = 0.0\ \mu$m and $\alpha = \gamma = 0°$. Four curves are plotted in the figure. The most remarkable feature of the graphs is their symmetry, i.e. $Q_{\text{ext}}(d) = Q_{\text{ext}}(-d)$. Attention should be paid to the fact that, when the displacement d separating the two origins is zero, the eccentric sphere should reduce to a concentric sphere system. Therefore, the extinction efficiencies keep the same for different incidence angles at the midposition $d = 0$ as observed in figure 5.

4. Conclusions

We have studied the interaction between a Gaussian beam and an eccentric sphere in the framework of the generalized Lorenz–Mie theory. By using the spherical vector wavefunctions, the incident beam is expanded in the general case of oblique illumination. The simulations are validated for plane wave scattering by an eccentric sphere and shaped beam scattering by a coated sphere, which agree with those published in the literature. The extinction efficiencies as a function of displacement distance d for a glycerol droplet containing a glass inclusion are also given. As a result, this approach provides a practical tool for calculating scattering of a Gaussian beam by an eccentric sphere with arbitrary orientation. Based

Table 1. Comparison of efficiency factors of coated sphere illuminated by a plane wave predicted by LMT and our code. $\lambda = 3.0\ \mu$m, $m_1 = 1.409 - 0.1747$i, $m_2 = 1.59 - 0.66$i, $m_0 = 1.0 - 0.0$i, $w_0 = 200\ \mu$m, $x_0 = y_0 = z_0 = 0.0\ \mu$m.

Radius (μm)	LMT	Our method ($d = 0$)
$a = 6.265$	$Q_{\text{ext}} = 2.328\,03$	$Q_{\text{ext}} = 2.328\,04$
$b = 0.171$	$Q_{\text{sca}} = 1.143\,41$	$Q_{\text{sca}} = 1.143\,41$
$a = 5.5$	$Q_{\text{ext}} = 2.344\,81$	$Q_{\text{ext}} = 2.344\,79$
$b = 1.5$	$Q_{\text{sca}} = 1.132\,27$	$Q_{\text{sca}} = 1.132\,25$
$a = 3.5$	$Q_{\text{ext}} = 2.583\,25$	$Q_{\text{ext}} = 2.583\,25$
$b = 2.0$	$Q_{\text{sca}} = 1.284\,85$	$Q_{\text{sca}} = 1.284\,81$

on this work, the Gaussian beam scattering by an eccentric sphere could be studied next.

It is worthwhile to point out that though a Gaussian beam is studied in this paper, the theory is also suitable for other beams by changing the BSCs.

Appendix A. Vector wavefunctions

We provide the vector wavefunctions used in this paper:

$$\bar{\mathbf{m}}^{(i)}_{nm,j} = [\mathrm{i}m z^{(i)}_n \pi^{|m|}_n(\theta_j)\mathbf{e}_\theta - z^{(i)}_n \tau^{|m|}_n(\theta_j)\mathbf{e}_\phi]\exp(\mathrm{i}m\phi_j), \quad (A.1)$$

$$\bar{\mathbf{n}}^{(i)}_{nm,j} = \frac{1}{k_j r_j}\left[n(n+1)z^{(i)}_n P^{|m|}_n(\theta_j)\mathbf{e}_\mathrm{r} + \frac{\mathrm{d}}{\mathrm{d}r_j}(r_j z^{(i)}_n)\tau^{|m|}_n(\theta_j)\mathbf{e}_\theta + \mathrm{i}m\frac{\mathrm{d}}{\mathrm{d}r_j}(r_j z^{(i)}_n)\pi^{|m|}_n(\theta_j)\mathbf{e}_\phi\right]\exp(\mathrm{i}m\phi_j), \quad (A.2)$$

where $z^{(i)}_n = z^{(i)}_n(kr)$ are the ith-kind spherical Bessel functions and $P^{|m|}_n(\theta)$ are the associated Legendre functions. The angular functions $\pi^{|m|}_n$ and $\tau^{|m|}_n$ are defined by

$$\pi^{|m|}_n(\theta) = \frac{1}{\sin\theta}P^{|m|}_n(\cos\theta), \qquad \tau^{|m|}_n(\theta) = \frac{\mathrm{d}}{\mathrm{d}\theta}P^{|m|}_n(\cos\theta). \quad (A.3)$$

The relationship between the vector wavefunctions in GLMT and those of Ngo $\mathbf{M}^{(i)}_{nm,j}$ and $\mathbf{N}^{(i)}_{nm,j}$ [15] are

$$\bar{\mathbf{m}}^{(i)}_{nm,j} = \Upsilon^m_n \mathbf{M}^{(i)}_{nm,j}, \quad (A.4)$$

$$\bar{\mathbf{n}}^{(i)}_{nm,j} = \Upsilon^m_n \mathbf{N}^{(i)}_{nm,j}, \quad (A.5)$$

where

$$\Upsilon^m_n = [\mathrm{sgn}(m)]^m\sqrt{\frac{2(n+|m|)!}{(2n+1)(n-|m|)!}}, \quad (A.6)$$

$\mathrm{sgn}(m)$ denotes the sign of m. This is due to the fact that the associated Legendre function in GLMT formulation is expressed in terms of $P^{|m|}_n$ instead of $\tilde{P}^m_n$ while we have the following relationship:

$$\tilde{P}^m_n(\cos\theta) = \sqrt{\frac{(2n+1)(n-m)!}{2(n+m)!}}P^m_n(\cos\theta), \quad (A.7)$$

and

$$P^{-m}_n(\cos\theta) = (-1)^m\frac{(n+m)!}{(n-m)!}P^m_n(\cos\theta), \quad (A.8)$$

between them. The advantage of this convention is that the BSCs $g^m_{n,TM}$ and $g^m_{n,TE}$, which are determined only by the characteristics of the beam, represent the profile of the incident beam. For instance, all the BSCs are unity for a plane wave, while the BSCs as a function of n are Gaussian for an on-axis Gaussian beam.

Appendix B. Coefficients of translational addition theorem

The coefficients of the translational addition theorem are given by

$$\bar{A}^m_{nn'} = \Gamma^m_{nn'}A^m_{nn'}, \qquad \bar{B}^m_{nn'} = \Gamma^m_{nn'}B^m_{nn'}, \quad (B.1)$$

with

$$\Gamma^m_{nn'} = \sqrt{\frac{(2n'+1)(n'-|m|)!(n+|m|)!}{(2n+1)(n-|m|)!(n'+|m|)!}}, \quad (B.2)$$

and

$$A^m_{nn'} = C^m_{nn'} - \frac{kd}{n'+1}\sqrt{\frac{(n'-m+1)(n'+m+1)}{(2n'+1)(2n'+3)}}C^m_{n,n'+1} - \frac{kd}{n'}\sqrt{\frac{(n'-m)(n'+m)}{(2n'-1)(2n'+1)}}C^m_{n,n'-1}, \quad (B.3)$$

$$B^m_{nn'} = -\frac{\mathrm{i}kmd}{n'(n'+1)}C^m_{n,n'}, \quad (B.4)$$

where $C^m_{n,n'}$ are scalar translation coefficients. Recursion expressions for these coefficients can be derived using the method of Bobbert and Vlieger [3]. The initial values are given by

$$C^0_{0,n'} = \sqrt{2n'+1}\,j_{n'}(kd), \quad (B.5)$$

$$C^0_{-1,n'} = -\sqrt{2n'+1}\,j_{n'}(kd), \quad (B.6)$$

$$C^0_{n+1,n'} = \frac{1}{2n+1}\sqrt{\frac{2n+3}{2n'+1}}\left[n'\sqrt{\frac{2n+1}{2n'-1}}C^0_{n,n'-1} + n\sqrt{\frac{2n'+1}{2n-1}}C^0_{n-1,n'} - (n'+1)\sqrt{\frac{2n+1}{2n'+3}}C^0_{n,n'+1}\right], \quad (B.7)$$

and the recursion relation is

$$\sqrt{(n-m+1)(n+m)(2n'+1)}C^m_{n,n'} = \sqrt{(n'-m+1)(n'+m)(2n'+1)}C^{m-1}_{n,n'} - kd\sqrt{\frac{(n'-m+2)(n'-m+1)}{(2n'+3)}}C^{m-1}_{n,n'+1} - kd\sqrt{\frac{(n'+m)(n'+m-1)}{(2n'-1)}}C^{m-1}_{n,n'-1}. \quad (B.8)$$

References

[1] Barton J P 1997 Electromagnetic-field calculations for a sphere illuminated by a higher-order Gaussian beam. I. Internal and near-field effects *Appl. Opt.* **36** 1303–11

[2] Barton J P and Alexander D R 1989 Fifth-order corrected electromagnetic field components for fundamental Gaussian beam *J. Appl. Phys.* **66** 2800–2

[3] Bobbert P A and Vlieger J 1986 Light scattering by a sphere on a substrate *Physica* A **137** 209–41
[4] Borghese F, Denti P, Saija R and Sindoni O I 1992 Optical properties of spheres containing a spherical eccentric inclusion *J. Opt. Soc. Am.* A **9** 1327–35
[5] Cruzan O R 1962 Translational addition theorems for spherical vector wavefunctions *Q. Appl. Math.* **20** 33–40
[6] Davis L W 1979 Theory of electromagnetic beams *Phys. Rev.* A **19** 1177–9
[7] Debye P 1909 Der Lichtdruck auf Kugeln von beliebigem material *Ann. Phys., Lpz.* **4** 57–136
[8] Fikioris J G and Uzunoglu N K 1979 Scattering from an eccentrically stratified dielectric sphere *J. Opt. Soc. Am.* A **69** 1359–66
[9] Friedman B and Russek J 1954 Addition theorems for spherical waves *Q. Appl. Math.* **12** 13–23
[10] Gouesbet G and Grehan G 2000 Generalized Lorenz–Mie theory for a sphere with an eccentrically located-spherical inclusion *J. Mod. Opt.* **47** 821–37
[11] Gouesbet G, Grehan G and Maheu B 1990 A localized interpretation to compute all the coefficients g_n^m in the generalized Lorenz–Mie theory *J. Opt. Soc. Am.* A **7** 998–1007
[12] Gouesbet G, Maheu B and Grehan G 1988 Light scattering from a sphere arbitrarily located in a Gaussian beam, using a Bromwich formulation *J. Opt. Soc. Am.* A **5** 1427–43
[13] Lorenz L 1890 Lysbevaegelsen i og uden for en af plane Lysbolger belyst Kulge *Vidensk. Selsk. Skr.* **6** 1–62
[14] Mie G 1908 Beitrage zur optik truber medien speziell kolloidaler metallosungen *Ann. Phys., Lpz.* **25** 377–452
[15] Ngo D, Videen G and Chylek P 1996 A Fortran code for the scattering of EM-waves by a sphere with a nonconcentric spherical inclusion *Comput. Phys. Commun.* **1077** 94–112
[16] Onofri F, Grehan G and Gouesbet G 1995 Electromagnetic scattering from a multilayered sphere located in an arbitrary beam *Appl. Opt.* **34** 7113–24
[17] Ngo D 1994 Light scattering from a sphere with a nonconcentric spherical inclusion *PhD Dissertation* Dept of Physics, New Mexico State University, Las Cruces
[18] Ren K F 1995 Diffusion des faisceaux feuille laser par une particule spherique et applicationsaux ecoulements diphasiques *PhD Thesis* Rouen University, France
[19] Ren K F, Grehan G and Gouesbet G 1992 Localized approximation of generalized Lorenz–Mie theory: faster algorithm for computations of the beam shape coefficients *Part. Part. Syst. Charact.* **9** 144–50
[20] Ren K F, Grehan G and Gouesbet G 1997 Scattering of a Gaussian beam by an infinite cylinder in the framework of generalized Lorenz–Mie theory: formulation and numerical results *J. Opt. Soc. Am.* A **14** 3014–25
[21] Stein S 1961 Additions theorems for spherical wavefunctions *Q. Appl. Math.* **19** 15–24
[22] Xu F, Ren K F and Cai X-S 2007 Expansion of arbitrarily oriented, located and shaped beam in spheroidal coordinates *J. Opt. Soc. Am.* A **24** 109–18
[23] Xu F, Ren K F, Cai X-S, Gouesbet G and Grehan G 2007 Generalized Lorenz–Mie theory for arbitrarily oriented, located and shaped beam scattering by a homogeneous spheroid *J. Opt. Soc. Am.* A **24** 119–31